DOI: 10.1002/ejic.200900128

Spectroscopic Characterization and Conformational Properties of *S*-(Fluoroformyl)-*O*-(acetyl) Thioperoxide and *S*-(Fluoroformyl)-*O*-(trifluoroacetyl) Thioperoxide

Marlene Cuaquira Reina,[a][‡] Carlos O. Della Védova,[a,b] Sonia E. Ulic,*[a,c] Helge Willner,[d] and Heinz Oberhammer[e]

Keywords: Sulfur / Matrix isolation / Pyrolysis / Vibrational spectroscopy / Conformation analysis / Quantum chemistry

The conformational properties of FC(O)SOC(O)CH$_3$ and FC(O)SOC(O)CF$_3$ were studied by vibrational spectroscopy [IR (gas phase, Ar matrix), Raman (liquid phase)] and quantum chemical calculations (B3LYP and MP2 methods). For both compounds the *syn-gauche-syn* conformer with synperiplanar orientation of both carbonyl C=O bonds with respect to the S–O bond, and *gauche* orientation around the S–O bond (C_1 symmetry) is the most stable structure [73(5) % for FC(O)SOC(O)CH$_3$ and 82(5) % for FC(O)SOC(O)CF$_3$]. For FC(O)SOC(O)CH$_3$ two more conformers are observed in the Ar-matrix spectra, 18(5) % *syn-trans-syn* with *trans* orientation around the S–O bond [ϕ(C–S–O–C) = 180°, C_2 symmetry] and 9(5) % *anti-gauche-syn* with the FC(O) group oriented *anti* with respect to the S–O bond. The experimental free energy differences for these most stable forms of FC(O)SOC(O)CH$_3$ are $\Delta G° = G°_{(syn\text{-}trans\text{-}syn)} - G°_{(syn\text{-}gauche\text{-}syn)} = 0.83(17)$ kcal mol^{-1} and $\Delta G° = G°_{(anti\text{-}gauche\text{-}syn)} - G°_{(syn\text{-}gauche\text{-}syn)} = 1.27(35)$ kcal mol^{-1}, respectively. These values are well reproduced by the B3YLP/aug-cc-pVTZ method (0.76 and 1.23 kcal mol^{-1}), but not by the MP2 approximation (2.72 and 1.28 kcal mol^{-1}) For FC(O)SOC(O)CF$_3$ only one more stable conformer, 18(5) % *anti-gauche-syn*, is observed. The experimental free energy difference between both rotamers of FC(O)SOC(O)CF$_3$, $\Delta G° = G°_{(anti\text{-}gauche\text{-}syn)} - G°_{(syn\text{-}gauche\text{-}syn)} = 0.90(17)$ kcal mol^{-1}, is reproduced very well by the B3YLP/6-311++G** method (0.82 kcal mol^{-1}) and reasonably well by B3LYP/aug-cc-pVTZ (1.17 kcal mol^{-1}) and MP2/6-31G* (1.23 kcal mol^{-1}) calculations.

(© Wiley-VCH Verlag GmbH & Co. KGaA, 69451 Weinheim, Germany, 2009)

Introduction

A fundamental concept in chemistry is that a group of linked atoms can exhibit a set of characteristic geometric and chemical properties and this is particularly useful for understanding the chemistry of biological macromolecules.[1–5] Some inherent differences between sulfur and oxygen atoms are reflected in the properties of S- and O-esters as a result of the lower electronegativity of sulfur and its reduced tendency to form double bonds as compared to oxygen.[6] For example, the alkaline hydrolysis of thioesters [R^{1}C(O)SR^2] is more favored than the hydrolysis of the corresponding esters [R^{1}C(O)OR^2].[7]

For a comparison between conformational properties of thioesters and esters, we became interested in compounds possessing a R^{1}C(O)SOC(O)R^2 connectivity, which belong to the class of sulfenic acid esters or thioperoxides, R^{1}SOR^2. They are structurally related to peroxides (R^{1}OOR^2) and disulfides (R^{1}SSR^2), characterized mostly by a *gauche* conformation around the S–O, O–O, and S–S bonds. This preferred conformation can be explained by taking into account anomeric effects.[8–10] However, some sulfenic esters of the type R^{1}SOC(O)R^2 exhibit a *trans* conformation as the second stable form at room temperature, which has been identified by IR spectroscopy[10,11] and gas electron diffraction (GED).[11] This planar structure is possibly stabilized by the mesomeric effect (one sp^2 hybridized atom attached to the S–O bond).

Moreover, thioperoxides CF$_3$SOCF$_3$[12] and CH$_3$SOCH$_3$[13] were observed and spectroscopically characterized in argon matrices after photoisomerization of CF$_3$S(O)CF$_3$ and CH$_3$S(O)CH$_3$, respectively. The dihedral angle in CF$_3$SOCF$_3$[12] [ϕ(C–S–O–C) = 105°] is closer to that in the corresponding disulfide, CF$_3$SSCF$_3$[14] [ϕ(C–S–

---

[a] CEQUINOR Facultad de Ciencias Exactas, Universidad Nacional de La Plata,
47 esq. 115, (1900) La Plata, Buenos Aires, República Argentina
E-mail: sonia@quimica.unlp.edu.ar
[b] Laboratorio de Servicios a la Industria y al Sistema Científico (UNLP-CIC-CONICET) Departamento de Química, Facultad de Ciencias Exactas, Universidad Nacional de La Plata,
Camino Centenario, Gonnet, Buenos Aires, República Argentina
[c] Departamento de Ciencias Básicas, Universidad Nacional de Luján,
Rutas 5 y 7 (6700) Luján, Buenos Aires, República Argentina
[d] Bergische Universität Wuppertal,
Gaußstraße 20, 42119 Wuppertal, Germany
[e] Institut für Physikalische und Theoretische Chemie, Universität Tübingen,
Auf der Morgenstelle 8, 72076 Tübingen, Germany

[‡] This work is part of the PhD thesis of M. C. R., who is a doctoral fellow of the Regional Program DAAD of Chemistry, Argentina.

S–C) = 104(4)°] and than that in the peroxide CF_3OOCF_3[15] [ϕ(C–O–O–C) = 123(4)°]. Angles near 100° were also observed in sulfenic esters possessing $R^1SOC(O)$-R^2 structures, such as in $CCl_3SOC(O)CH_3$[10] [ϕ(C–S–O–C) = 105.9(15)°], $CF_3SOC(O)CH_3$[11] [ϕ(C–S–O–C) = 100(4)°], $CF_3SOC(O)CF_3$[11] [ϕ(C–S–O–C) = 101(3)°], and $CCl_3SOC(O)CF_3$[16] [ϕ(C–S–O–C) = 108.5°]. Otherwise, in sulfenic esters with two C=O groups, the dihedral angle around the S–O bond is smaller than 90°, as in FC(O)-$SOC(O)CF_3$[17] [ϕ(C–S–O–C) = 75(3)°] and $CF_3C(O)SOC$-$(O)CF_3$[18] [ϕ(C–S–O–C) = 77°].

It is also interesting to take into account the theoretical study of Gregory and Jenks[19] about the S–O bond dissociation energy of thioperoxides. The value found for CH_3S–OCH_3 (64 kcal mol^{-1}) is much closer to the bond dissociation energy in disulfides, CH_3S–SCH_3 (72 kcal mol^{-1}), than to that in peroxides, CH_3O–OCH_3 (37 kcal mol^{-1}). This is attributed to reduced lone-pair repulsion and to the electronegativity difference between S and O. Both effects increase the bond enthalpy of S–O relative to O–O. A structural parameter of particular interest in these compounds is the torsional angle around the S–O, S–S, or O–O bonds.

In order to obtain additional experimental and theoretical information about the structural and conformational behavior of sulfenic esters with $R^1C(O)SOC(O)R^2$ structure, we present in this publication the study of FC(O)-$SOC(O)CH_3$ and $FC(O)SOC(O)CF_3$. These compounds were fully characterized by infrared, Raman, UV, and NMR (^{1}H, ^{19}F) spectroscopy. The geometric structure of $FC(O)SOC(O)CH_3$ was determined by theoretical methods (MP2/6-31G*, B3YLP/6-311++G**, and B3YLP/aug-cc-pVTZ), whereas the conformational properties of FC(O)-$SOC(O)CF_3$ were previously determined by experimental methods.[17] Recently, $FC(O)SOC(O)CH_3$ was analyzed by photoelectron spectroscopy.[20]

Results

Quantum Chemical Calculations

There are several possible conformations for FC(O)-$SOC(O)CH_3$ and $FC(O)SOC(O)CF_3$, depending on the torsional angle around the S–O bond and on the orientation of the C=O bonds of the FC(O) and $CH_3C(O)$ or $CF_3C(O)$ groups (torsion around C–S and O–C bonds). Each of the C=O groups can be *syn* or *anti* relative to the S–O bond, and the orientation around of the S–O bond can be *gauche* or *trans*. This leads to eight possible conformers for both $FC(O)SOC(O)CH_3$ and $FC(O)SOC(O)CF_3$. If we describe them by the orientation around the C–S, S–O, and O–C bonds, these possible conformers are *syn-gauche-syn*, *anti-gauche-syn*, *syn-gauche-anti*, *anti-gauche-anti*, *syn-trans-syn*, *anti-trans-syn*, *syn-trans-anti*, and *anti-trans-anti* (see Figure 1 for $FC(O)SOC(O)CH_3$).

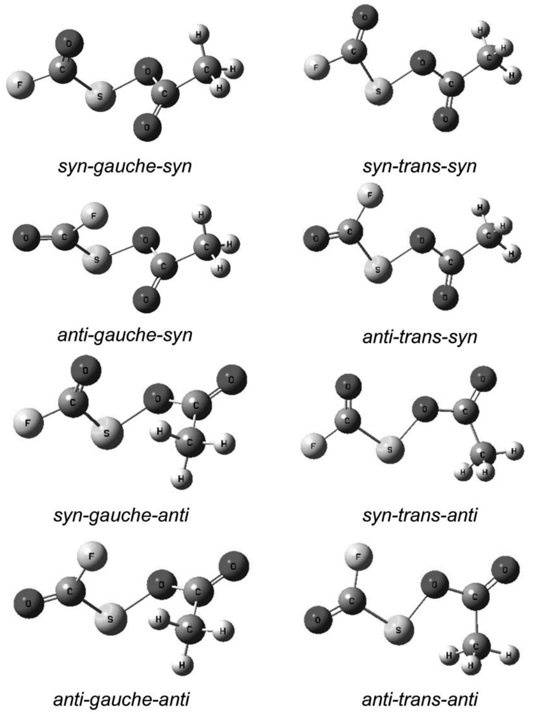

syn-gauche-syn *syn-trans-syn*

anti-gauche-syn *anti-trans-syn*

syn-gauche-anti *syn-trans-anti*

anti-gauche-anti *anti-trans-anti*

Figure 1. Schematic representation of possible conformers of $FC(O)SOC(O)CH_3$.

In order to estimate the energy difference between the conformers, a scan of the potential energy surface was performed by rotating the torsional angles ϕ(O=C–S–O), ϕ(C–S–O–C), and ϕ(S–O–C=O) in steps of 30° by using the DFT/B3LYP method. The potential energy curves for the dihedral angles ϕ(O=C–S–O) and ϕ(S–O–C=O) obtained from 0 to 180° with the 6-31G* basis set are shown in Figure 2 for $FC(O)SOC(O)CH_3$ and in Figure 3 for FC(O)-$SOC(O)CF_3$. The four curves possess minima at 0 and 180° for ϕ(O=C–S–O) and ϕ(S–O–C=O), which correspond to *syn* and *anti* orientation of the carbonyl groups. The potential energy curves for the dihedral angle ϕ(C–S–O–C), obtained for $FC(O)SOC(O)CH_3$ with different methods at the MP2/6-31G*, B3LYP/6-31G*, and B3LYP/6-311G(2df,pd) levels (Figure 4), show two equivalent minima around 80 and 280° (*gauche* orientation) and an additional but ex-

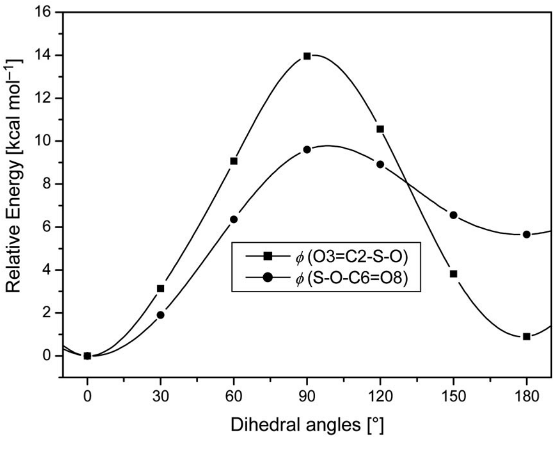

Figure 2. Calculated potential curves for internal rotation around the C_{sp^2}–S and O–C_{sp^2} bond in $FC(O)SOC(O)CH_3$ by using the B3LYP/6-31G* method (atom numbering is depicted in Figure 5).

tremely flat minimum at 180° (*trans* orientation). Further single-point calculations at MP2/6-311++G** and MP4/6-31G* levels, however, result in an imaginary frequency at 180°, that is, the structures with *trans* orientation around the S–O bond are predicted to be transition states.

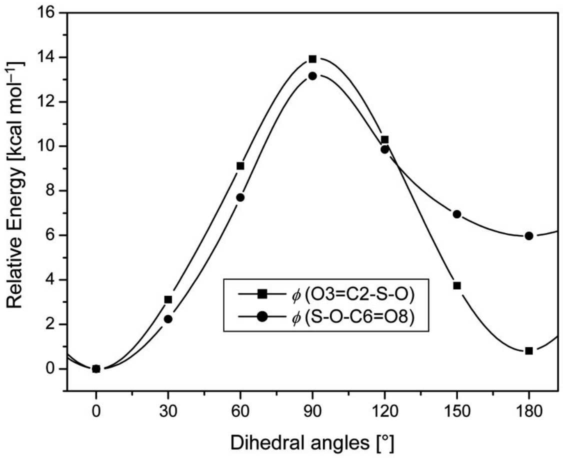

Figure 3. Calculated potential curves for internal rotation around the C_{sp^2}–S and O–C_{sp^2} bond in FC(O)SOC(O)CF_3 by using the B3LYP/6-31G* method (atom numbering is depicted in Figure 5).

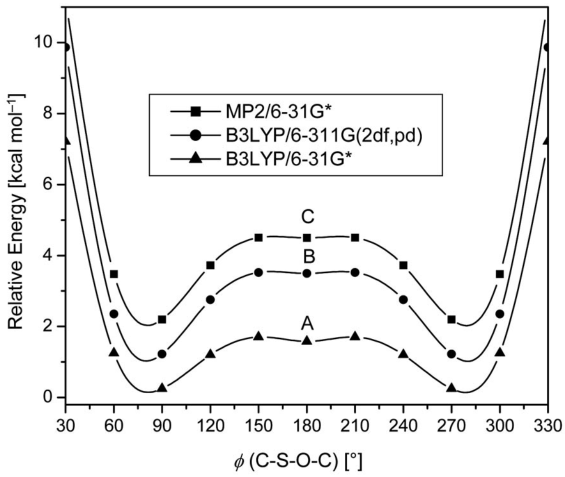

Figure 4. Calculated potential curves for internal rotation around the S–O bond in FC(O)SOC(O)CH_3. (A) B3LYP/6-31G*, (B) B3LYP/6-311G(2df,pd), (C) MP2/6-31G* methods. Curves B and C are shifted by 1 and 2 kcal mol^{-1}, respectively.

Optimization of the eight feasible conformations with B3LYP/6-311++G**, B3LYP/aug-cc-pVTZ, and MP2/6-31G* methods result in six stable structures (see Table 1). For *syn-trans-anti* and *anti-trans-anti* conformers, one imaginary frequency is obtained. Computed relative energies, free energies, and calculated C=O vibrational frequencies and their intensities for the six stable conformers are summarized in Table 1. The computed relative energies and free energies depend considerably on the computational method. The B3LYP/6-311++G** and B3LYP/aug-cc-pVTZ methods both predict the existence of three conformers with $\Delta G° < 2.0$ kcal mol^{-1}, *syn-gauche-syn*, *anti-gauche-syn*, and *syn-trans-syn*. In contrast, the MP2/6-31G* approximation gives only two forms with $\Delta G° <$ 2.0 kcal mol^{-1}, *syn-gauche-syn* and *anti-gauche-syn*.

As for FC(O)SOC(O)CH_3, all three methods predict the *syn-gauche-syn* conformer with C_1 symmetry (Figure 1) to be the most stable one. The *syn-trans-syn* (C_S symmetry) and *anti-gauche-syn* (C_1 symmetry) forms are predicted to possess higher free energies by 0.76 and 1.23 kcal mol^{-1} (B3LYP/aug-cc-pVTZ), respectively. The potential energy

Table 1. Calculated relative energies, free energies (kcal mol^{-1}), and ν(C=O) vibrational frequencies [cm^{-1}] for FC(O)SOC(O)CH_3.

Conformer[a]	Method of calculation	ΔE	$\Delta G°$	ν(FC=O)[c]	ν(CH_3C=O)[c]
syn-gauche-syn	MP2/6-31G*	0.00	0.00	1900 (219)	1872 (147)
	B3LYP/6-311++G**	0.00	0.00	1892 (333)	1853 (254)
	B3LYP/aug-cc-pVTZ	0.00	0.00	1877 (302)	1847 (236)
anti-gauche-syn	MP2/6-31G*	1.37	1.28	1877 (307)	1872 (140)
	B3LYP/6-311++G**	1.25	0.97	1860 (478)	1852 (231)
	B3LYP/aug-cc-pVTZ	1.44	1.23	1847 (395)	1845 (256)
syn-trans-syn[b]	MP2/6-31G*	3.26	2.72	1908 (222)	1834 (201)
	B3LYP/6-311++G**	1.67	0.90	1901 (346)	1806 (326)
	B3LYP/aug-cc-pVTZ	1.33	0.76	1883 (318)	1799 (300)
anti-trans-syn[b]	MP2/6-31G*	4.74	4.09	1868 (324)	1833 (166)
	B3LYP/6-311++G**	2.82	1.94	1852 (493)	1806 (277)
	B3LYP/aug-cc-pVTZ	2.69	2.20	1838 (458)	1798 (246)
syn-gauche-anti	MP2/6-31G*	6.82	7.19	1890 (262)	1875 (168)
	B3LYP/6-311++G**	5.88	6.32	1887 (395)	1870(275)
	B3LYP/aug-cc-pVTZ	5.18	5.54	1874 (389)	1861 (252)
anti-gauche-anti	MP2/6-31G*	8.15	8.45	1878 (45)	1870 (485)
	B3LYP/6-311++G**	7.13	7.29	1871 (53)	1858 (769)
	B3LYP/aug-cc-pVTZ	6.60	6.71	1862 (123)	1845 (651)

[a] See Figure 1. [b] Different multiplicities (m = 2 for *gauche* and m = 1 for *trans* structures) were taken into account in $\Delta G°$ values. [c] The calculated IR intensities (km mol^{-1}) are given in parentheses.

© 2009 Wiley-VCH Verlag GmbH & Co. KGaA, Weinheim

Table 2. Calculated geometric parameters for the *syn-gauche-syn* conformer of $FC(O)SOC(O)CH_3$ and electron diffraction data of $FC(O)SOC(O)CF_3$.

Parameters[a]	B3LYP[b]		MP2/6-31G*[b]	GED[b,c]
	6-311++G**	aug-cc-pVTZ		
C2–F1	1.359	1.355	1.360	1.335(3)
C2=O3	1.178	1.178	1.195	1.179(3)
C2–S4	1.770	1.765	1.758	1.771(6)
S4–O5	1.690	1.672	1.689	1.647(5)
O5–C6	1.400	1.398	1.407	1.382(16)
C6–C7	1.502	1.499	1.499	1.524(10)
C6=O8	1.192	1.190	1.206	1.188(3)
C7–H9	1.088	1.088	1.089	1.326(3)[d]
F1–C2=O3	123.4	123.3	124.0	125.2(21)
F1–C2–S4	106.8	106.7	106.8	103.3(13)
O3=C2–S4	129.8	129.9	129.2	131.5(19)
C2–S4–O5	98.5	98.9	97.5	101.9(19)
S4–O5–C6	118.1	117.8	115.3	114.3(12)
O5–C6–C7	108.6	108.9	108.1	104.0(27)
O5–C6=O8	123.3	123.1	123.6	130.0(22)
C7–C6=O8	128.1	127.8	128.3	126.0(32)
C6–C7–H9	109.1	109.1	108.9	
H9–C7–H10	109.9	109.8	110.0	108.0(6)[e]
F1–C2–S4–O5	176.7	176.5	177.9	
O3=C2–S4–O5	–3.0	–3.1	–2.1	–2.6
C2–S4–O5–C6	82.3	82.9	74.1	75.2(28)
S4–O5–C6=O8	–0.1	0.3	–0.1	–2.2
O5–C6–C7–H9	–173.3	–173.8	–174.1	
O8=C6–C7–H9	7.3	6.6	7.2	

[a] Distances [Å], angles [°]. For atom numbering see Figure 5. [b] Not refined. A negative value implies shortening of the O3···O8 distance upon torsion around the S–C and O–C bonds. [c] Parameters obtained by gas electron diffraction (GED) of $FC(O)SOC(O)CF_3$. [d] Bond length C7–F9. [e] Angle F9–C7–F10.

curve for the dihedral angle ϕ(C–S–O–C) of $FC(O)SOC(O)CF_3$ was reported previously.[17] Calculations at the B3LYP/aug-cc-pVTZ level for $FC(O)SOC(O)CF_3$ predicted the *syn-gauche-syn* conformer, with C_1 symmetry, to be the most stable one, whereas the *anti-gauche-syn* form is higher in free energy by 1.18 kcal mol^{-1}.

Thus, the *syn-gauche-syn* conformation is preferred for both $FC(O)SOC(O)CH_3$ and $FC(O)SOC(O)CF_3$. Table 2 summarizes geometric parameters of the *syn-gauche-syn* conformer of $FC(O)SOC(O)CH_3$ calculated with the MP2/6-31G*, B3LYP/6-31++G**, and B3LYP/aug-cc-pVTZ methods in order to compare these results with electron diffraction data of $FC(O)SOC(O)CF_3$ (Figure 5).[17]

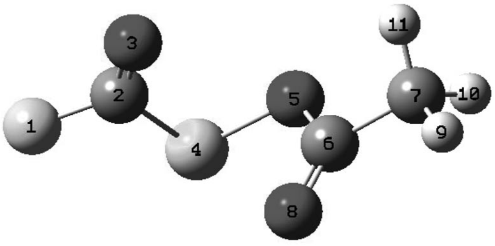

Figure 5. Molecular model and atom numbering for the most-stable conformer (*syn-gauche-syn*) at room temperature for $FC(O)SOC(O)CH_3$ and $FC(O)SOC(O)CF_3$.

Spectroscopic Characterization

The ^1H and ^{19}F NMR spectra of $FC(O)SOC(O)CH_3$ each show one singlet with chemical shift values of 2.3 and 50.8 ppm, respectively, corresponding to the CH_3 group and the FC(O) group. For comparison, the ^{19}F NMR spectrum of $FC(O)SOC(O)CF_3$ exhibits two singlets at 50.4 and –73.1 ppm with an intensity ratio of 1:3 assigned to the FC(O) and $CF_3C(O)$ groups, respectively.

The UV/Vis spectra of $FC(O)SOC(O)CH_3$ and $FC(O)SOC(O)CF_3$ are both characterized by three absorptions with maxima at 199, 210, and 294 nm and at 203, 208, and 273 nm, respectively. An assignment was made by comparison with $CF_3C(O)SOC(O)CF_3$.[18] The two bands at lower wavelengths correspond to $\pi \rightarrow \pi^*$ transitions, originating from the C(O)O and C(O)S chromophores, whereas the third band at 294 and 273 nm, respectively, is due to the S–O group.

Vibrational Analyses

The infrared (gas) and Raman (liquid) spectra of $FC(O)SOC(O)CH_3$ and $FC(O)SOC(O)CF_3$ are shown in Figures 6 and 7, respectively. The assignment of bands was performed by comparison with calculated frequencies, their relative intensities, and with experimentally obtained wavenumbers of related molecules such as $FC(O)SSC(O)CF_3$,[21] $FC(O)SCl$,[22] $FC(O)SCH_3$,[23] $CCl_3SOC(O)CH_3$,[10] $CF_3SOC(O)CH_3$,[24] $CF_3SOC(O)CF_3$,[24] and $CF_3C(O)SOC(O)CF_3$.[18] Observed and calculated (B3LYP/6-31++G**) frequencies for the *syn-gauche-syn* conformer of $FC(O)SOC(O)CH_3$ and $FC(O)SOC(O)CF_3$ were fully assigned by a force-field analysis using the program Asym40[25] and are listed in Tables 3 and 4, respectively. The observed frequency shifts between different conformers as well as the individual sign of each shift are in good agreement with results obtained from quantum chemical calculations (B3LYP/6-311++G**).

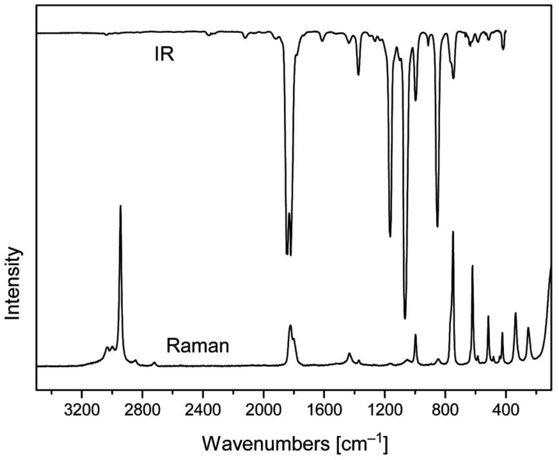

Figure 6. IR (gas) and Raman (liquid) spectra of FC(O)SOC(O)-CH_3 at room temperature.

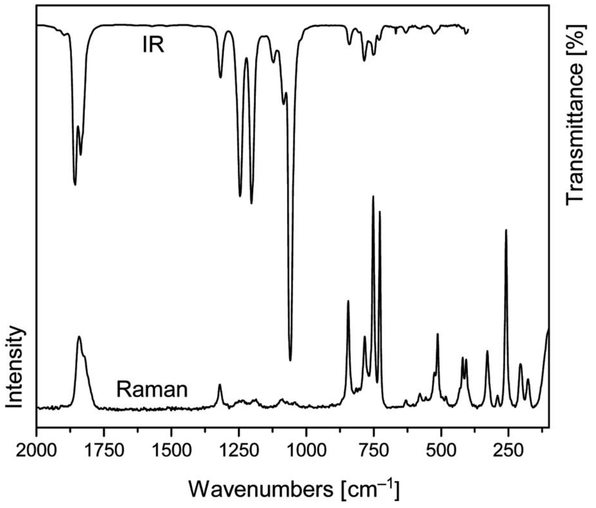

Figure 7. IR (gas) and Raman (liquid) spectra of FC(O)SOC(O)-CF_3 at room temperature.

Table 3. Experimentally determined (IR, Raman) and calculated vibrational wavenumbers of FC(O)SOC(O)CH_3.

Mode	IR (gas)[a]	Raman (liquid)[a]	IR (Ar matrix)	B3LYP/6-311++G**[b]		Assignment[c]
	syn-gauche-syn	*syn-gauche-syn*	*syn-gauche-syn*	*syn-gauche-syn*	*syn-trans-syn*	
ν_1	3038 vw	3033 w		3160 (2)	3161 (2)	$\nu_s(CH_3)$
ν_2	3002 vw	2996 w		3119 (1)	3119 (1)	$\nu_{as}(CH_3)$
ν_3	2957 vw	2945 vs		3054 (<1)	3056 (<1)	$\nu_{as}(CH_3)$
ν_4	1848[d] sh.		1839[d]	1892 (333)	1901 (346)	ν(C=O2)
	1842 vs	1821 m	1836			
ν_5	1821 vs	1801 w	1814 1778[d]	1853 (254)	1806 (326)	ν(C=O8)
ν_6				1471 (12)	1472 (11)	$\delta_{as}(CH_3)$
ν_7	1437 w	1433 w	1433	1470 (14)	1471 (13)	$\delta_{as}(CH_3)$
ν_8	1374 w	1372 vw	1368	1396 (27)	1398 (24)	$\delta_s(CH_3)$
ν_9			1179^{d}	1172 (206)	1217 (301)	ν(O–C)/ν(C–C)/ $\rho_s(CH_3)$
	1164 s	1164 sh.	1160			
ν_{10}			1064	1064 (5)	1064 (7)	$\rho_{as}(CH_3)$
ν_{11}	1066 vs	1051 vw	1058 1045[d]	1034 (484)	1022 (496)	ν(C–F)/δ(F–C=O)
ν_{12}	998 m	997 m	990	996 (61)	1006 (125)	ν(C–C)/$\rho_s(CH_3)$
ν_{13}	852 s	846 w	848	842 (201)	921 (33)	ν(S–O)/ν(O–C)
ν_{14}	748 w	749 vs	768	753 (15)	753 (31)	ν(S–O)
ν_{15}			746	742 (19)	743 (35)	ν(C–S)
ν_{16}	634 vw	620 s	635	631 (7)	627 (7)	[e]oop(C=O3)
ν_{17}				616 (1)	598 (3)	δ(O–C=O)
ν_{18}	582 vw	586 vw	581	589 (6)	594 (9)	[e]oop(C=O8)/$\rho_s(CH_3)$
ν_{19}	512 vw	516 m	515	508 (6)	486 (1)	ν(C–S)/δ(F–C=O)
ν_{20}	418 vw	423 m	420	416 (8)	421 (7)	δ(O–C–C)/δ(F–C–S)
ν_{21}		336 m		324 (1)	312 (1)	δ(O–C–C)
ν_{22}		253 m		245 (7)	212 (2)	δ(O=C–S)/δ(C–S–O)
ν_{23}				233 (3)	184 (4)	δ(S–O–C)
ν_{24}				96 (<1)	110 (8)	τ(C–S)
ν_{25}				87 (1)	82 (1)	τ(C–C)
ν_{26}				64 (1)	33 (<1)	τ(S–O)/τ(O–C)
ν_{27}				53 (2)	20 (2)	τ(S–O)/τ(C–C)/τ(O–C)

[a] Abbreviations: vs, very strong; s, strong; m, medium; w, weak; vw, very weak. [b] Calculated IR intensities (km mol^{-1}) in parentheses. [c] The greek letters ν, δ, τ, and ρ represent stretching, deformation, torsion, and rocking modes. [d] Corresponding bands of the *syn-trans-syn* conformer. [e] Out of plane.

© 2009 Wiley-VCH Verlag GmbH & Co. KGaA, Weinheim

Table 4. Experimentally determined (IR, Raman) and calculated vibrational wavenumbers of FC(O)SOC(O)CF$_3$.

Mode	IR (gas)[a]	Raman (liquid)[a]	IR (Ar matrix)	B3LYP/6-311++G**[b]		Assignment[c]
	syn-gauche-syn	*syn-gauche-syn*	*syn-gauche-syn*	*syn-gauche-syn*	*anti-gauche-syn*	
ν_1	1857 s	1842	1850 1834[d]	1908 (347)	1877 (234)	ν(C=O3)
ν_2	1836 s	1823	1827 1818[d]	1875 (226)	1871 (462)	ν(C=O8)
ν_3	1318 m	1320	1320	1285 (56)	1285 (51)	ν(C–C)/ν_s(CF$_3$)/δ_s(CF$_3$)
ν_4	1245 s		1241	1209 (321)	1208 (326)	ν_{as}(CF$_3$)/δ_{as}(CF$_3$)
ν_5	1203 s		1182	1158 (288)	1159 (342)	ν_{as}(CF$_3$)/δ_{as}(CF$_3$)
ν_6	1083 m		1172[d] 1151	1077 (228)	1102 (410)	ν(C(sp^2)–F)/ν(O–C)/δ_s(CF$_3$)
ν_7	1062 vs		1049	1036 (751)	1057 (406)	ν(O–C)/δ(O=C–S)
ν_8	840 w	844		845 (15)	846 (14)	δ(F–C=O)
ν_9	785 w	783	776	768 (17)	772 (14)	[e]oop (C=O8)
ν_{10}	751 w	752	756	757 (42)	745 (58)	ν (S–O)
ν_{11}	729 w	727	743	742 (34)	742 (48)	ρ_s(CF$_3$)
ν_{12}				711 (1)	704 (2)	ρ_{as}(CF$_3$)
ν_{13}	630 w	630		626 (9)	627 (9)	[e]oop (C=O2)/δ (S–C–C)
ν_{14}				564 (<1)	562 (<1)	δ_{as}(CF$_3$)
ν_{15}	525 w	524 513[d]		522 (9)	519 (9)	δ_{as}(CF$_3$)/δ (F–C=O)
ν_{16}				504 (4)	475 (10)	ν(C–S)/δ(O=C–S)
ν_{17}		420[d] 407		413 (3)	425 (4)	δ(O=C–O)
ν_{18}				400 (4)	407 (<1)	δ(F–C–S)
ν_{19}		328		325 (3)	326 (1)	ρ(F–C=O)
ν_{20}				288 (3)	287 (5)	ρ_s(CF$_3$)
ν_{21}		259		249 (10)	250 (10)	δ(C–S–O)
ν_{22}		205		194 (1)	190 (<1)	δ(C–O–S)
ν_{23}		177		164 (<1)	159 (<1)	δ(O–C–C)
ν_{24}				88 (<1)	79 (<1)	τ(C–S)
ν_{25}				61 (<1)	56 (1)	τ(C–C)
ν_{26}				47 (<1)	44 (<1)	τ(S–O)/τ(O–C)
ν_{27}				22 (<1)	19 (<1)	τ(S–O)/τ(O–C)/τ(C–C)

[a] Abbreviations: vs, very strong; s, strong; m, medium; w, weak; vw, very weak. [b] Calculated IR intensities (km mol^{-1}) in parentheses. [c] The greek letters ν, δ, τ, and ρ represent stretching, deformation, torsion, and rocking modes. [d] Corresponding bands of the *anti-gauche-syn* conformer. [e] Out of plane.

FC(O)SOC(O)CH$_3$

In the IR (gas) spectrum of FC(O)SOC(O)CH$_3$ three bands are observed in the CH stretching region at 3038, 3002, and 2957 cm^{-1}, which are assigned to ν_{as}(CH$_3$), ν_{as}(CH$_3$), and ν_s(CH$_3$) by comparison with values obtained from CCl$_3$SOC(O)CH$_3$[10] and CF$_3$SOC(O)CH$_3$.[24] Typical shapes and intensities of the CH$_3$ group are observed in the Raman spectrum of the liquid, and the bands at 3033, 2996, and 2945 cm^{-1} are attributed to the same modes.

The ν(C=O) stretching vibration of carbonyl compounds are particularly sensitive to conformational properties. The bands at 1842 and 1821 cm^{-1} in the IR spectrum of the gas can be assigned to the FC(O) and CH$_3$C(O) groups of the *syn*-*gauche*-*syn* conformer (C_1 symmetry) by taking into account results from similar compounds and of theoretical calculations. These modes are observed at 1825 and 1801 cm^{-1} in the Raman spectrum of the liquid. An additional shoulder at 1848 cm^{-1} (gas phase) can be attributed to the FC(O) group of the *syn*-*trans*-*syn* form (C_S symmetry). A difference value $\Delta\nu$(C=O) of 6 cm^{-1} calculated by B3LYP/aug-cc-pVTZ for the FC(O) group between *syn*-*trans*-*syn* and *syn*-*gauche*-*syn* agrees very well with the experimental result, whereas a difference of 30 cm^{-1} is predicted for the *anti*-*gauche*-*syn* conformer.

More information about the conformational properties can be derived from the C=O stretching region (Figure 8) of the Ar matrix IR spectra recorded at different temperatures of the matrix/gas mixture prior to deposition. The positions and intensities of the C=O vibrations of the three low-energy conformers, *syn*-*gauche*-*syn*, *anti*-*gauche*-*syn*, and *syn*-*trans*-*syn*, are shown in the simulated spectra (Figure 9) by assuming a 1:1:1 contribution. In total, four bands in the C=O region are obtained. The observed IR band intensities (Figure 8) are in good agreement with those obtained from quantum chemical calculations (MP2/6-31G*, B3LYP/6-311++G**, and B3LYP/aug-cc-pVTZ methods). The theoretical frequencies of the two C=O vibrations in the *anti*-*gauche*-*syn* conformer calculated with B3LYP/aug-cc-pVTZ are close to each other, FC(O) at 1847 cm^{-1} (exp. 1814 cm^{-1}) and CH$_3$C(O) at 1845 cm^{-1} (exp. 1814 cm^{-1}). The former two vibrations overlap with the corresponding CH$_3$C(O) vibration of the *syn*-*gauche*-*syn* conformer (calcd. 1847 cm^{-1}, exp. 1814 cm^{-1}). Thus, the strong peak at 1814 cm^{-1} in the Ar matrix IR spectrum has to be assigned to these three vibrations. The FC(O) vibrations of the *syn*-*gauche*-*syn* conformer at 1836 cm^{-1} (calcd. 1877 cm^{-1}) and the *syn*-*trans*-*syn* conformer at 1839 cm^{-1} (calcd. 1883 cm^{-1}) are very close to each other, but resolved in the IR matrix

© 2009 Wiley-VCH Verlag GmbH & Co. KGaA, Weinheim

spectrum (Figure 8). The separate peak at 1778 cm^{-1} (calcd. 1799 cm^{-1}) is attributed to the C=O stretching vibration of the $CH_3C(O)$ group of the *syn-trans-syn* form. Although the quantum chemically obtained frequencies are too high by about 30–40 cm^{-1}, the calculated shifts agree well with the experimental values.

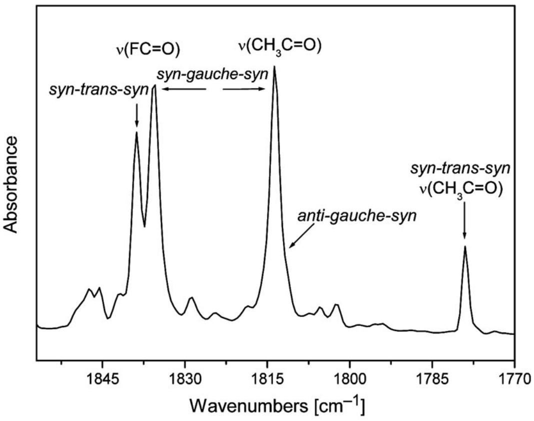

Figure 8. Carbonyl stretching region of the Ar matrix IR spectrum of $FC(O)SOC(O)CH_3$. The temperature of the spray-on nozzle was held at 20 °C.

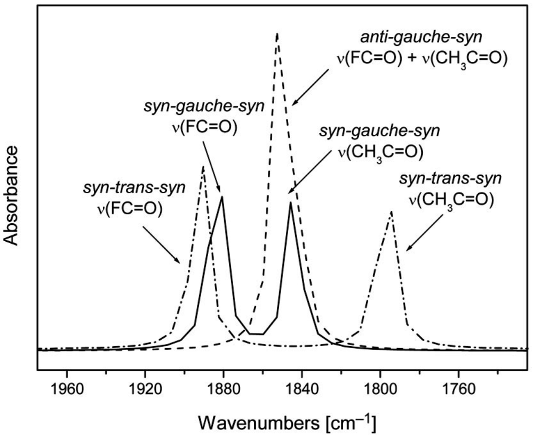

Figure 9. Simulated carbonyl stretching region of the IR spectra calculated at the B3LYP/aug-cc-pVTZ level for the *syn-gauche-syn* (——), *syn-trans-syn* (–•–•–), and *anti-gauche-syn* (– – –) conformers of $FC(O)SOC(O)CH_3$.

The C=O stretching region of the Ar matrix IR spectra demonstrates the presence of at least two conformers, *syn-gauche-syn* and *syn-trans-syn*. Taking, however, into account the relative areas of the four C=O bands and their predicted intensities, the following equilibrium mixture of conformers can be derived: 73% *syn-gauche-syn*, 18% *syn-trans-syn*, and 9% *anti-gauche-syn*. Error limits due to uncertainties in the experimentally determined areas and calculated intensities are estimated to be 5%. The values correspond to the equilibrium mixture at room temperature, that is, the temperature of the gas prior to deposition in the matrix. They are reproduced very well by the B3LYP/aug-cc-pVTZ method, which predicts 71% *syn-gauche-syn*, 20% *syn-trans-syn*, and 9% *anti-gauche-syn*. The temperature dependence of the matrix IR spectra also confirms the above assignment. The intensities of bands corresponding to the most abundant *syn-gauche-syn* conformer decrease with increasing temperature and those corresponding to the less abundant *syn-trans-syn* and *anti-gauche-syn* conformers increase. The experimentally determined conformational composition at room temperature (Ar matrix) corresponds to relative free energies of 0.83(17) kcal mol^{-1} for *syn-trans-syn* and 1.27(35) kcal mol^{-1} for *anti-gauche-syn*, both higher in energy than the *syn-gauche-syn* conformer. These values are in good agreement with the relative free energies predicted by the B3LYLP/aug-cc-pVTZ method (0.00, 0.76, and 1.23 kcal mol^{-1}, respectively). Although this method reproduces the experimentally determined conformational composition fairly well, the MP2 method fails to predict correct values (Table 1).

The bands at 1058 cm^{-1} (high intensity) and 1045 cm^{-1} (low intensity) in the Ar matrix IR spectrum were assigned to the ν(C_{sp^2}–F) vibrational modes of the *syn-gauche-syn* and the *syn-trans-syn* conformer, respectively.

The S–O group, a characteristic feature of sulfenic esters, is observed as a weak band at 748 cm^{-1} in the IR spectrum of the gas and as a very strong band at 749 cm^{-1} in the Raman spectrum of the liquid. It was assigned by taking into account the similar band position in other S–O containing compounds such as $CF_3C(O)SOC(O)CF_3$[18] (783 cm^{-1}, IR), $CF_3SOC(O)CF_3$[24] (765 cm^{-1}, Raman), $CF_3SOC(O)CH_3$[24] (762 cm^{-1}, Raman), and $CCl_3SOC(O)CH_3$[10] (757 cm^{-1}, Raman).

When the $FC(O)SOC(O)CH_3$/Ar mixture was heated to temperatures higher than 20 °C and deposited as a matrix at 15 K, new bands appeared in the IR spectra. They were assigned to $FC(O)SCH_3$,[26] $CH_2{=}C{=}O$,[27] CO_2,[28,29] OCS,[30] and CO.[31] Hence, the thermal decarboxylation of $FC(O)SOC(O)CH_3$ results in the formation of *syn* and *anti* $FC(O)SCH_3$;[26] the corresponding C=O bands were observed at 1802 and 1805 cm^{-1}, respectively. Figure 10 shows the ν(C–H) stretching region between 3080 and 2900 cm^{-1} of the Ar matrix IR spectra after deposition of the gas mix-

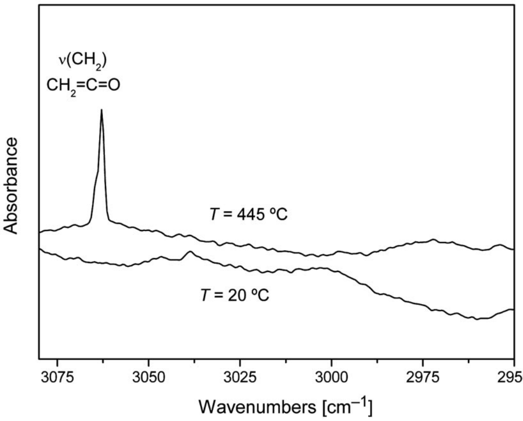

Figure 10. CH_3 stretching region of the matrix IR spectra taken from $FC(O)SOC(O)CH_3$/Ar mixtures and their thermolysis products. The temperature of the spray-on nozzle was held at 20 and 445 °C, respectively.

ture at 20 and 445 °C. The presence of $CH_2=C=O$ [ν(C–H), 3062 cm^{-1}] after pyrolysis may indicate the formation of the hitherto unknown FC(O)SOH. The characteristic overtone of the δ(SOH) (Figure 11) could be assigned to the band at 2274 cm^{-1} in comparison with some reported data.[32,33] Scheme 1 shows a possible mechanism for the thermal decomposition of $FC(O)SOC(O)CH_3$.

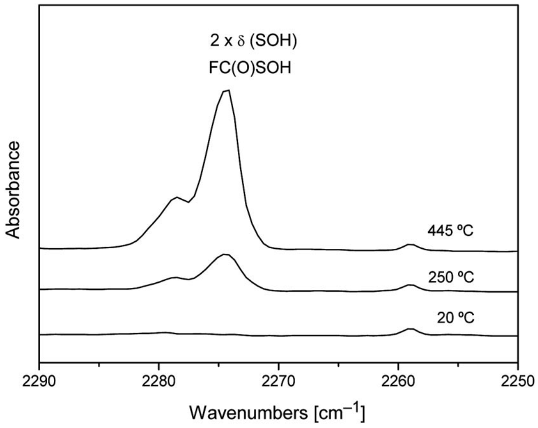

Figure 11. Overtone region of the SOH deformation of the matrix IR spectra taken from $FC(O)SOC(O)CH_3$/Ar mixtures and their thermolysis products. The temperature of the spray-on nozzle was held at 20, 250, and 445 °C, respectively.

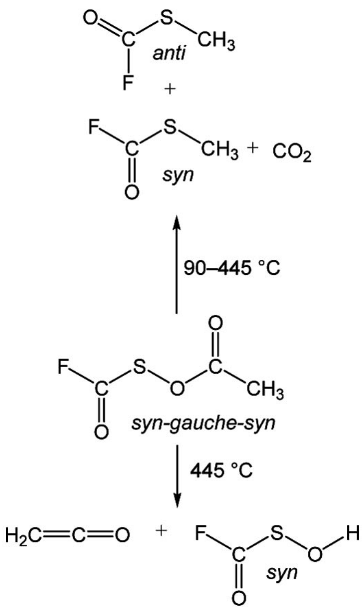

Scheme 1. Proposed mechanism for the thermal decomposition of $FC(O)SOC(O)CH_3$ diluted in Ar gas.

Figure 12 shows the carbonyl stretching region of the matrix IR spectra of $FC(O)SOC(O)CH_3$ between 1850 and 1760 cm^{-1} recorded after UV irradiation (high-pressure Hg lamp) for 20 and 60 min. New bands appeared after photolysis, which were assigned to $FC(O)SCH_3$,[26] CH_3SF,[26] $CH_2=S\cdots HF$,[26] CO_2,[28,29] OCS,[30] CS_2,[30] and CO.[31] The photodecarboxylation of $FC(O)SOC(O)CH_3$ results in $FC(O)SCH_3$, which looses CO to form CH_3SF identified by its S–F stretching vibration at 807 cm^{-1}. After longer irradiation times, a new band at 3511 cm^{-1} was observed, which is assigned to HF. The unusual low frequency for this species probably corresponds to a HF molecule complexed to $CH_2=S$.[26] Scheme 2 presents a possible mechanism for the photochemical decomposition of $FC(O)SOC(O)CH_3$. The photoevolution from *syn* $FC(O)SCH_3$ to $FSCH_3$ is similar to that reported in the literature.[26]

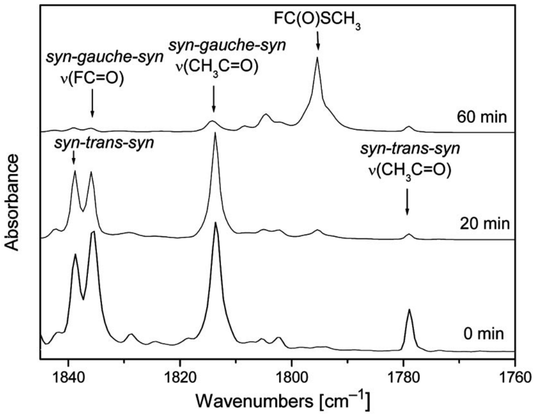

Figure 12. Carbonyl stretching region of the matrix IR spectra of $FC(O)SOC(O)CH_3$ recorded after different UV irradiation times.

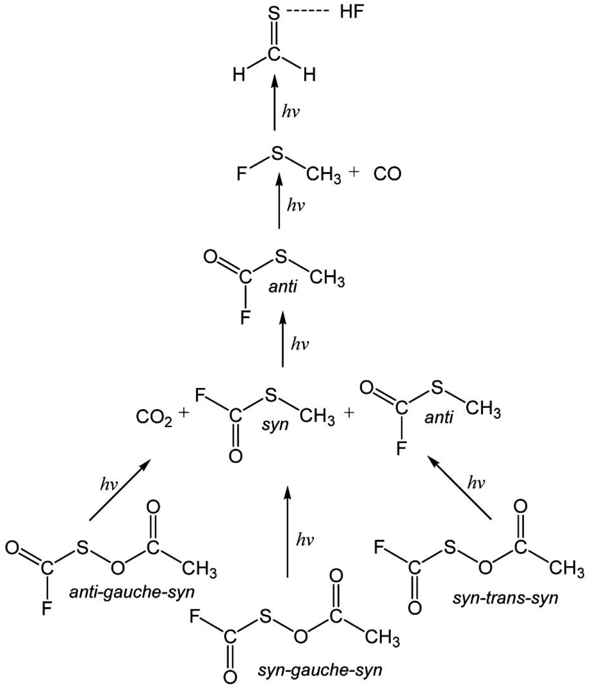

Scheme 2. Proposed mechanism for the photolysis of FC(O)-$SOC(O)CH_3$ isolated in Ar matrices.

$FC(O)SOC(O)CF_3$

Ab initio and density functional B3LYP calculations indicate that the *syn-gauche-syn* conformer is more stable than *anti-gauche-syn* conformer at room temperature, and the Ar matrix IR spectra are consistent with this prediction. Frequencies at 1857 and 1836 cm^{-1} in the IR spectrum of the gas and at 1842 and 1823 cm^{-1} in the Raman spectrum of the liquid are assigned to the C=O stretching vibration of the FC(O) and $CF_3C(O)$ groups. Ar matrix IR spectra were recorded from $FC(O)SOC(O)CF_3/Ar$ mixtures that were kept at higher temperatures prior to their deposition as an Ar matrix at 15 K. These spectra reveal an equilibrium of conformers exhibiting four bands in the C=O stretching region. Two intense bands at 1850 and 1827 cm^{-1} arising from the FC(O) and the $CH_3C(O)$ substituent, respectively, were assigned to the main *syn*-*gauche*-*syn* conformer, whereas two additional weak bands at 1834 cm^{-1} [FC(O)] and 1818 cm^{-1} [$CF_3C(O)$] were attributed to *anti*-*gauche*-*syn*. The relative intensities of these bands increase with increasing temperature of the gas mixture prior to deposition. The shifts Δν(C=O) observed for the FC(O) and the $CF_3C(O)$ substituents of the two conformers come up to 16 and 9 cm^{-1}, respectively. Because, however, B3LYP/aug-cc-pVTZ calculated frequency shifts of both carbonyl groups result in nearly identical values of 16 and 6 cm^{-1} for *anti*-*gauche*-*syn* but in values of 6 and 35 cm^{-1} for *syn*-*trans*-*syn*, the second conformer possesses an *anti*-*gauche*-*syn* and not a *syn*-*trans*-*syn* structure. From the relative areas of the C=O stretching vibrations from their calculated intensities a composition of 82(5)% *syn*-*gauche*-*syn* and 18(5)% *anti*-*gauche*-*syn* is derived. The error limits are estimated from uncertainties in the experimentally determined areas and in the calculated intensities. The composition corresponds to $\Delta G° = G°_{(anti\text{-}gauche\text{-}syn)} - G°_{(syn\text{-}gauche\text{-}syn)} = 0.90(17)$ kcal mol^{-1}. This result is in perfect agreement with a former GED experiment[17] [$\Delta G° = 0.91(24)$ kcal mol^{-1}] and it is reproduced well by DFT calculations affording free energies $\Delta G°$ of 0.82 kcal mol^{-1} with the B3LYP/6-311++G** of 1.17 kcal mol^{-1} with the B3LYP(aug-cc-pVTZ) and of 1.23 kcal mol^{-1} with the MP2/6-31G* approximation.

In the IR spectrum of the gas, three CF stretching bands are observed at 1318 [$\nu_s(CF_3)$], 1245, and 1203 cm^{-1} [$\nu_{as}(CF_3)$]. These bands are very weak in the Raman spectrum of the liquid.

Bands at 1172 and 1151 cm^{-1} in Ar matrix IR spectrum were assigned to the $\nu(C_{sp^2}\text{–}F)$ mode of the *anti*-*gauche*-*syn* and the *syn*-*gauche*-*syn* conformer, respectively.

The S–O stretching vibration of $FC(O)SOC(O)CF_3$ is observed as a weak band in the IR spectrum of the gas at 751 cm^{-1} and as a strong band at 752 cm^{-1} in the Raman spectrum of the liquid. The assignment takes into account similar values of related molecules.[10,18,24]

Conclusions

The vibrational spectra of the $FC(O)SOC(O)CH_3$ and $FC(O)SOC(O)CF_3$ molecules reveal that both compounds exist in the gas phase as a mixture of three and two conformers, respectively, showing contributions of 73(5)% [$FC(O)SOC(O)CH_3$] and 82(5)% [$FC(O)SOC(O)CF_3$] of *syn*-*gauche*-*syn*. In $FC(O)SOC(O)CH_3$, the second stable form exhibits the *syn*-*trans*-*syn* structure [18(5)%], which differs only in the orientation at the S–O bond, and the third conformer has an *anti*-*gauche*-*syn* structure [9(5)%] with an *anti* orientation of the FC(O) group. In $FC(O)SOC(O)CF_3$, the *syn*-*trans*-*syn* form was not observed and the second conformer [18(5)%] shows the *anti*-*gauche*-*syn* structure.

In the case of $FC(O)SOC(O)CH_3$, the experimentally determined conformational composition at room temperature corresponds to free energies of 0.83(17) kcal mol^{-1} for *syn*-*trans*-*syn* and 1.27(35) kcal mol^{-1} for *anti*-*gauche*-*syn* relative to the most stable *syn*-*gauche*-*syn* conformer. These values are reproduced perfectly by calculations at the B3LYP/aug-cc-pVTZ level, which predict 0.76 and 1.23 kcal mol^{-1}, respectively. In $FC(O)SOC(O)CF_3$ the contribution of the less stable *anti*-*gauche*-*syn* conformer [18(5)%] corresponds to a relative free energy $\Delta G°$ of 0.90(17) kcal mol^{-1}. In this case the experimental value is reproduced very well by the B3LYP/6-311++G** method ($\Delta G° = 0.82$ kcal mol^{-1}) and reasonably well by B3LYP/aug-cc-pVTZ ($\Delta G° =$ 1.17 kcal mol^{-1}) and by MP2/6-31G* calculations ($\Delta G° =$ 1.23 kcal mol^{-1}).

Generally, the substituents at the S–O and S–S single bonds adopt a *gauche* orientation with dihedral angles close to 90° as in $FC(O)SOC(O)CF_3$[17] [ϕ(C–S–O–C) = 75.2(28)°] or $FC(O)SSC(O)CF_3$[21] [ϕ(C–S–S–C) = 77.7(2)°]. Quantum chemical calculations predict similar values for the *syn*-*gauche*-*syn* conformer (C_1 symmetry) of FC(O)-$SOC(O)CH_3$ [ϕ(C–S–O–C) = 82.3°]. Those angles are typically observed in sulfenic esters with two carbonyl substituents such as FC(O), $C(O)CH_3$, or $C(O)CF_3$. Two different features become apparent from this rather limited number of examples (see Table 5): the dihedral angle depends on the steric requirement of the substituent and on the hybridization (sp^3 or sp^2) of the carbon atom attached. The angle increases with increasing steric requirements of the substituents, as, for example, in HSOH [ϕ(H–S–O–H) = 91.3°] and CF_3SOCF_3 [ϕ(C–S–O–C) = 105.0°] or $CF_3SOC(O)CH_3$ [ϕ(C–S–O–C) = 100.0(4)°] and $CCl_3SOC(O)CH_3$ [ϕ(C–S–O–C) = 105.9(15)°]. Exchange of a substituent by a different one with an sp^2 hybridized carbon atom slightly decreases the dihedral angle, as, for example, CF_3SOCF_3 [ϕ(C–S–O–C) = 105.0°] and $CF_3SOC(O)CF_3$ [ϕ(C–S–O–C) = 101.0(3)°]. Thioperoxides possessing substituents with two sp^2 hybridized carbon atoms have dihedral angles near 90° or smaller, as, for example, $FC(O)SOC(O)CF_3$ [ϕ(C–S–O–C) = 75.2(28)°] or $CF_3(O)SOC(O)CF_3$ [ϕ(C–S–O–C) = 77°].

Studies of carbonylsulfenyl compounds with the general formula XC(O)SY have established the preference of the *syn* conformation at the C–S bond. In the case of sulfenic esters and disulfides (Y = OR or SR), the preferred mutual orientation of the C=O and S–Y bonds is *syn*[10,11,17,18,21] as well. It is also known that in thioperoxides (Y = OR) the *trans* conformation at the S–O bond may be a second stable form.[10,11] This phenomenon was observed by gas electron diffraction (GED) with $CF_3SOC(O)CH_3$[11] and $CF_3SOC(O)CF_3$[11] and by matrix IR spectroscopy with

Table 5. S–O bond lengths and dihedral angles in $R^1S–OR^2$.[a]

$R^1S–OR^2$	S–O	$\delta(R^1–S–O–R^2)$	Method
HS–OH[34]	1.662	91.3	CCSD(T)/cc-pCVQZ
$CF_3S–OCF_3$[12]	1.677	105.0	B3LYP/6-311++G(3df,3pd)
$CF_3S–OC(O)CH_3$[11]	1.659(4)	100(4)	GED
$CF_3S–OC(O)CF_3$[11]	1.663(5)	101(3)	GED
$CCl_3S–OC(O)CH_3$[10]	1.663(14)	105.9(15)	X-ray
$CCl_3S–OC(O)CF_3$[16]	1.694	108.5	B3LYP/6-311+G(3df)
$FC(O)S–OC(O)CF_3$[17]	1.647(5)	75.2(28)	GED
$FC(O)S–OC(O)CH_3$[b]	1.690	82.3	B3LYP/6-311++G**
$CF_3C(O)S–OC(O)CF_3$[18]	[c]	77	B3LYP/6-31G*
$CF_3C(O)O–SS–OC(O)CF_3$[35]	1.755	91.8	B3LYP/6-311G*
$CH_3C(O)O–SS–OC(O)CH_3$[36]	1.710	92.3	B3LYP/6-311++G(3df,3pd)

[a] Distances, [Å], angles [°]. [b] This work. [c] No data available.

$CCl_3SOC(O)CH_3$.[10] At low temperatures in the solid the latter compound exists only as the *gauche* conformer. These three compounds have one substituent with one sp^3-hybridized carbon atom (CF_3 or CCl_3) and a second one with a sp^2-hybridized carbon atom [$C(O)CH_3$ or $C(O)CF_3$]. In the present study, we report the first example of a thioperoxide exhibiting two carbonyl substituents, FC(O) and $CH_3C(O)$, for which also a *trans* conformer (*syn-trans-syn*) with a contribution of 18(5)% is observed. No conformer, however, with *trans* orientation at the S–O bond was observed in the vibrational spectra and in a previous GED study for the similar compound $FC(O)SOC(O)CF_3$.[17] The existence of a *trans* conformer in these thioperoxides may be due to mesomeric effects.

Experimental Section

General Procedure: Volatile materials were manipulated in a glass vacuum line equipped with a capacitance pressure gauge, three U-traps, and valves with PTFE stems (Young, London, UK). The pure compound was stored in flame-sealed glass ampoules (6 mm o.d.) under liquid nitrogen in a long-term Dewar vessel.

Synthesis: $FC(O)SOC(O)CF_3$ was synthesized by applying reported methods,[37] and $FC(O)SOC(O)CH_3$ was prepared by reaction of FC(O)SCl with $AgOC(O)CH_3$. The products were separated by "trap-to-trap" distillation, keeping traps at different temperatures. Pure $FC(O)SOC(O)CH_3$ and $FC(O)SOC(O)CF_3$ were retained as colorless liquids, and their purity were checked by IR and (^1H, ^{19}F) NMR spectroscopy.

Instrumentation

Vibrational Spectroscopy: Infrared (gas) spectra were recorded with a Bruker IFS 66v FTIR instrument, with a resolution of 1 cm^{-1} in the range 4000 to 400 cm^{-1}, using a gas cell with optical path length of 200 mm and Si windows (0.5 mm thick). Raman spectra of the liquid were measured with a Bruker RFS 100/S FT Raman spectrometer in the region 3500 to 100 cm^{-1} with 2 cm^{-1} resolution.

Matrix Isolation: The sample was placed into a small U-trap that was mounted in front of the matrix support and cooled to –82 °C. A stream of argon gas was passed over the sample in the U-trap, and the resulting mixtures of gaseous compound and argon (≈1:1000) were forced through a quartz tube with a nozzle of 1 mm i.d. that was electrically heated over a length of ≈15 mm. The nozzle was kept at temperatures of 20, 90, 250, 350, and 445 °C prior to deposition of the matrix gas mixture onto the matrix support, a rhodium-plated copper mirror cooled to ≈15 K by a He continuous flow cryostat. Details of the matrix apparatus has been described elsewhere.[38] For photolysis experiments, radiation from a 150 W mercury high-pressure lamp (TQ150, Haereus, Hanau, Germany) without cutoff filter was used over a period of 5 to 60 min. IR (Ar matrix) spectra of the deposits were recorded with a Bruker IFS 66v/s FTIR spectrometer in absorption/reflection mode with a resolution of 0.5 cm^{-1} in the range 4000 to 400 cm^{-1}.

UV Spectroscopy: UV/Vis spectra of the gaseous sample were recorded using a glass cell (10 cm optical path length) equipped with quartz windows in a Perkin–Elmer Lambda EZ210 spectrometer. The measurements were carried out in the spectral region 190 to 600 nm.

NMR Spectroscopy: ^1H and ^{19}F NMR spectra of samples filled into 5 mm NMR tubes with PTFE valves were recorded with a Bruker MSL 200 NMR spectrometer by using $CDCl_3$ as solvent and $(CH_3)_4Si$ as internal reference.

Theoretical Calculations: Calculations were performed by using the Gaussian 03 program package[39] applied with the ab initio (HF and MP2 methods) as well as the density function B3LYP approach. The basis sets 6-31G*, 6-311++G**, and aug-cc-pVTZ were used to optimize different conformers of $FC(O)SOC(O)CH_3$ and $FC(O)SOC(O)CF_3$. The potential functions for internal rotation around the C–S, S–O, and O–C bonds were derived by structure optimization at fixed dihedral angles. Vibrational frequency calculations were carried out to verify stationary points for both molecules. For the normal coordinate analysis, transformations of the ab initio Cartesian harmonic force constants to the molecule-fixed internal coordinate system were performed, as described by Hedberg and Mills and implemented in the ASYM40 program.[25] By using this procedure the potential energy distribution (PED) associated with each normal vibrational mode under the harmonic assumption was evaluated.

Acknowledgments

The authors thank the Deutscher Akademischer Austauschdienst, Germany (DAAD), Agencia Nacional de Promoción Científica y Técnica (ANPCYT), Consejo Nacional de Investigaciones Científicas y Técnicas (CONICET), Comisión de Investigaciones de la Provincia de Buenos Aires (CIC), and Facultad de Ciencias Exactas, Universidad Nacional de La Plata (UNLP). S. E. U. thanks Departamento de Ciencias Básicas de la Universidad Nacional de Luján for financial support and Dr. Mauricio F. Erben for helpful discussions. M. C. R. acknowledges the DAAD award. A special gratitude is owed by C. O. D. V. to DAAD, who generously spon-

© 2009 Wiley-VCH Verlag GmbH & Co. KGaA, Weinheim

sors the DAAD Regional Program of Chemistry for the República Argentina supporting Latin-American students to carry out Ph D studies in La Plata.

[1] C. F. Matta, R. F. W. Bader, *Proteins Struct., Funct., Genet.* **2000**, *40*, 310–329.
[2] C. F. Matta, R. F. W. Bader, *Proteins Struct., Funct., Genet.* **2002**, *48*, 519–538.
[3] C. F. Matta, R. F. W. Bader, *Proteins Struct., Funct., Genet.* **2003**, *52*, 360–399.
[4] M. L. Chodkiewicz, *J. Chem. Phys.* **2005**, *122*, 224107–224114.
[5] Y. A. Arnautova, A. Jagielska, H. A. Scheraga, *J. Phys. Chem. B* **2006**, *110*, 5025–5044.
[6] R. Hilal, A. M. El-Aaser, *Biophys. Chem.* **1985**, *22*, 145–150.
[7] J. P. Idoux, P. T. R. Hwang, C. K. Hancock, *J. Org. Chem.* **1973**, *38*, 4239–4243.
[8] D. R. Alleres, D. L. Cooper, T. P. Cunningham, J. Gerratt, P. B. Karadakov, M. Raimondi, *J. Chem. Soc. Faraday Trans.* **1995**, *91*, 3357–3362.
[9] J. Kirby, *The Anomeric Effect and Related Stereochemical Effects at Oxygen*, Springer, Berlin, **1983**.
[10] M. Cuaquira Reina, R. Boese, M. Ge, S. E. Ulic, H. Beckers, H. Willner, C. O. Della Védova, *J. Phys. Chem. A* **2008**, *112*, 7939–7946.
[11] S. E. Ulic, A. Kosma, C. Leibold, C. O. Della Védova, H. Willner, H. Oberhammer, *J. Phys. Chem. A* **2005**, *109*, 3739–3744.
[12] S. E. Ulic, S. von Ahsen, H. Willner, *Inorg. Chem.* **2004**, *43*, 5268–5274.
[13] M. Chen, R. Yang, R. Ma, M. Zhou, *J. Phys. Chem. A* **2008**, *112*, 7157–7161.
[14] C. J. Marsden, B. Beagley, *J. Chem. Soc. Faraday Trans. II* **1981**, *77*, 2213–2216.
[15] C. J. Marsden, L. S. Bartell, F. P. Diodati, *J. Mol. Struct.* **1977**, *39*, 253–262.
[16] L. Du, L. Yao, X. Zeng, M. Ge, D. Wang, *J. Phys. Chem. A* **2007**, *111*, 4944–4949.
[17] S. E. Ulic, A. Kosma, C. O. Della Védova, H. Willner, H. Oberhammer, *J. Phys. Chem. A* **2006**, *110*, 10201–10205.
[18] S. E. Ulic, C. O. Della Védova, A. Hermann, H.-G. Mack, H. Oberhammer, *Inorg. Chem.* **2002**, *41*, 5699–5705.
[19] D. D. Gregory, W. S. Jenks, *J. Org. Chem.* **1998**, *63*, 3859–3865.
[20] S. Tong, M. Ge, W. Wang, C. O. Della Védova, *J. Mol. Struct.* **2009**, *919*, 83–88.
[21] M. F. Erben, C. O. Della Védova, H. Willner, F. Trautner, H. Oberhammer, R. Boese, *Inorg. Chem.* **2005**, *44*, 7070–7077.
[22] C. O. Della Védova, A. Jubert, O. E. Piro, E. L. Varetti, P. J. Aymonino, *J. Fluorine Chem.* **1982**, *21*, 90–90.
[23] C. O. Della Védova, *J. Raman Spectrosc.* **1989**, *20*, 483–488.
[24] M. Cuaquira Reina, S. E. Ulic, C. O. Della Védova, unpublished results.
[25] L. Hedberg, I. M. Mills, *J. Mol. Spectrosc.* **2000**, *203*, 82–95.
[26] R. M. Romano, C. O. Della Védova, A. J. Downs, *Chem. Eur. J.* **2007**, *13*, 8185–8192.
[27] C. B. Moore, C. P. George, *J. Chem. Phys.* **1963**, *38*, 2816–2829.
[28] T. Svensson, B. Nelander, G. Karlström, *Chem. Phys.* **2001**, *265*, 323–333.
[29] H. Abe, H. Takeo, K. M. T. Yamada, *Chem. Phys. Lett.* **1999**, *311*, 153–158.
[30] M. Hawkins, M. J. Almond, A. J. Downs, *J. Phys. Chem.* **1985**, *89*, 3326–3334.
[31] H. Dubost, *Chem. Phys.* **1976**, *12*, 139–151.
[32] A. Königshofen, M. Behnke, M. Hoverath, J. Hahn, *Z. Anorg. Allg. Chem.* **1999**, *625*, 1778–1786.
[33] H. Beckers, S. Esser, T. Metzroth, M. Behnke, H. Willner, J. Gauss, J. Hahn, *Chem. Eur. J.* **2006**, *12*, 832–844.
[34] G. Winnewisser, F. Lewen, S. Thoswirth, M. Behnke, J. Hahn, J. Gauss, E. Herbst, *Chem. Eur. J.* **2003**, *9*, 5501–5510.
[35] X. Zeng, M. Ge, Z. Sun, D. Wang, *J. Phys. Chem. A* **2006**, *110*, 5685–5691.
[36] L. Du, L. Yao, M. Ge, *J. Phys. Chem. A* **2007**, *111*, 11787–11792.
[37] A. Haas, J. Helmbrecht, W. Klug, B. Koch, H. Reinke, J. Sommerhoff, *J. Fluorine Chem.* **1974**, *3*, 383–395.
[38] H. Schöckel, H. Willner, *Matrix-Isolated Molecules*, VCH, Weinheim, Germany, **1994**, p. 297.
[39] M. J. Frisch, G. W. Trucks, H. B. Schlegel, G. E. Scuseria, M. A. Robb, J. R. Cheeseman, J. A. Montgomery Jr, T. Vreven, K. N. Kudin, J. C. Burant, J. M. Millam, S. S. Iyengar, J. Tomasi, V. Barone, B. Mennucci, M. Cossi, G. Scalmani, N. Rega, G. A. Petersson, H. Nakatsuji, M. Hada, M. Ehara, K. Toyota, R. Fukuda, J. Hasegawa, M. Ishida, T. Nakajima, Y. Honda, O. Kitao, H. Nakai, M. Klene, X. Li, J. E. Knox, H. P. Hratchian, J. B. Cross, V. Bakken, C. Adamo, J. Jaramillo, R. Gomperts, R. E. Stratmann, O. Yazyev, A. J. Austin, R. Cammi, C. Pomelli, J. W. Ochterski, P. Y. Ayala, K. Morokuma, G. A. Voth, P. Salvador, J. J. Dannenberg, V. G. Zakrzewski, S. Dapprich, A. D. Daniels, M. C. Strain, O. Farkas, D. K. Malick, A. D. Rabuck, K. Raghavachari, J. B. Foresman, J. V. Ortiz, Q. Cui, A. G. Baboul, S. Clifford, J. Cioslowski, B. B. Stefanov, G. Liu, A. Liashenko, P. Piskorz, I. Komaromi, R. L. Martin, D. J. Fox, T. Keith, M. A. Al-Laham, C. Y. Peng, A. Nanayakkara, M. Challacombe, P. M. W. Gill, B. Johnson, W. Chen, M. W. Wong, C. Gonzalez, J. A. Pople, *Gaussian 03*, Revision D.01, Gaussian, Inc., Wallingford, CT, **2004**.

Received: February 5, 2009
Published Online: August 7, 2009

© 2009 Wiley-VCH Verlag GmbH & Co. KGaA, Weinheim